Petrology, Vol. 12, No. 4, 2004, pp. 330–347. Translated from Petrologiya, Vol. 12, No. 4, 2004, pp. 374–393.

Age and Duration of Svecofennian Plutono-Metamorphic Activity in the Ladoga Area, Southeastern Baltic Shield

Sh. K. Baltybaev, O. A. Levchenkov, N. G. Berezhnaya, L. K. Levskii, A. F. Makeev, and S. Z. Yakovleva

Institute of Precambrian Geology and Geochronology, Russian Academy of Sciences, nab. Makarova 2, St. Petersburg, 199034 Russia
e-mail: sb@sb2085.spb.edu

Received April 23, 2003

Abstract—The U–Pb system was examined in minerals of the main rock types from the Ladoga area: early- and synorogenic enderbites, diorites, syn- and late-orogenic K-granites, the leucosomes of migmatites, and their host garnet–cordierite and garnet–hypersthene gneisses. The peak of the granulite metamorphism was dated and the duration of each retrograde metamorphic stage was evaluated. The age of the Svecofennian plutono-metamorphic activity is constrained between 1.89–1.88 and 1.86–1.85 Ga. The geochemistry, morphology, and inner structure of the zircon and monazite of different genetic types are studied in detail to determine whether these minerals can be used as chronometers of each of the petrogenetic processes. The rocks crystallizing from melts (magmatic rocks and the leucosomes of migmatites) were determined to have similar U–Pb zircon and monazite ages. The Th/U ratios of monazite from the igneous rocks are generally higher than in this mineral of metamorphic and ultrametamorphic genesis. Age relations for two migmatite zones (sodic and potassic migmatites) in the Ladoga area are examined. The U–Pb system of monazite and zircon from migmatites and gneisses in the two migmatite zones suggest that they were produced simultaneously at 1871–1876 Ma.

INTRODUCTION

The Ladoga area is one of the rare metamorphic terranes made up of a great variety of metamorphic rocks, which were produced in the range from the lowest (greenschist facies) to highest (granulites) metamorphic grades (*Geologic Evolution...*, 1970). The metamorphic zoning in the Ladoga area can be regarded as a manifestation of a thermal dome of Svecofennian age. Although the area was thoroughly studies for a long time by many geologists (Kitsul, 1963; Predovskii *et al.*, 1967; Saranchina, 1972; Lobach-Zhuchenko *et al.*, 1974; Nagaitsev, 1974; Kazakov, 1976; Tugarinov and Bibikova, 1980; Morozov and Gaft, 1985; *Migmatization and Granite Formation...*, 1985; Kotov and Samorukova, 1990; Svetov and Sviridenko, 1992; Glebovitsky, 1993; and others), such issues as age correlations between magmatic, metamorphic, and ultrametamorphic processes, age constraints of the metamorphic *P–T* path, and correlations between endogenic activity in different zones of the Ladoga area remain known inadequately poorly. Our research was centered on reproducing the evolution of the thermal regime of the high-grade core of the zonal metamorphic complex (ZMC) by means of petrological and isotopic-geochronological study of rocks of different metamorphic stages.

GEOLOGICAL OVERVIEW

The study area is located in the northeastern termination of the Svecofennian belt, which trends for more than 400 km (Fig. 1, inset). The geotectonic setting of the Ladoga area is determined by its restriction to the boundary between the Karelia craton and island-arc complexes in Finland. In the past years, the area was subdivided into two domains: Northern (ND) and Southern (SD) (Baltybaev *et al.*, 2000). The ND belongs to the Sveco-Karelian pericratonic zone, and the SD affiliates with the Svecofennides proper, which have no Archean granitic basement.

The ND is characterized by the development of mantled gneissic domes with an Archean gneiss–granite basement in the cores. The metamorphic grade in the ND increases southward from the greenschist to amphibolite facies, the magmatic activity is insignificant.

The SD is a block metamorphosed to the granulite facies and containing numerous intrusions of gabbro, enderbites, tonalite, and granites. This block is regarded as the core of the ZMC. The SD is thrust over the ND along a thick zone of gently inclined faults (Baltybaev *et al.*, 1996).

The SD is subdivided into two zones: Lahdenpohja and Priozersk (Fig. 1, inset) (Shul'diner *et al.*, 1997a). This subdivision was based on the compositional zoning of the SD metasediments. The Lahdenpohja zone is dominated by Ca–Na graywackes in association with marlaceous rocks and, perhaps, calc–alkaline volca-

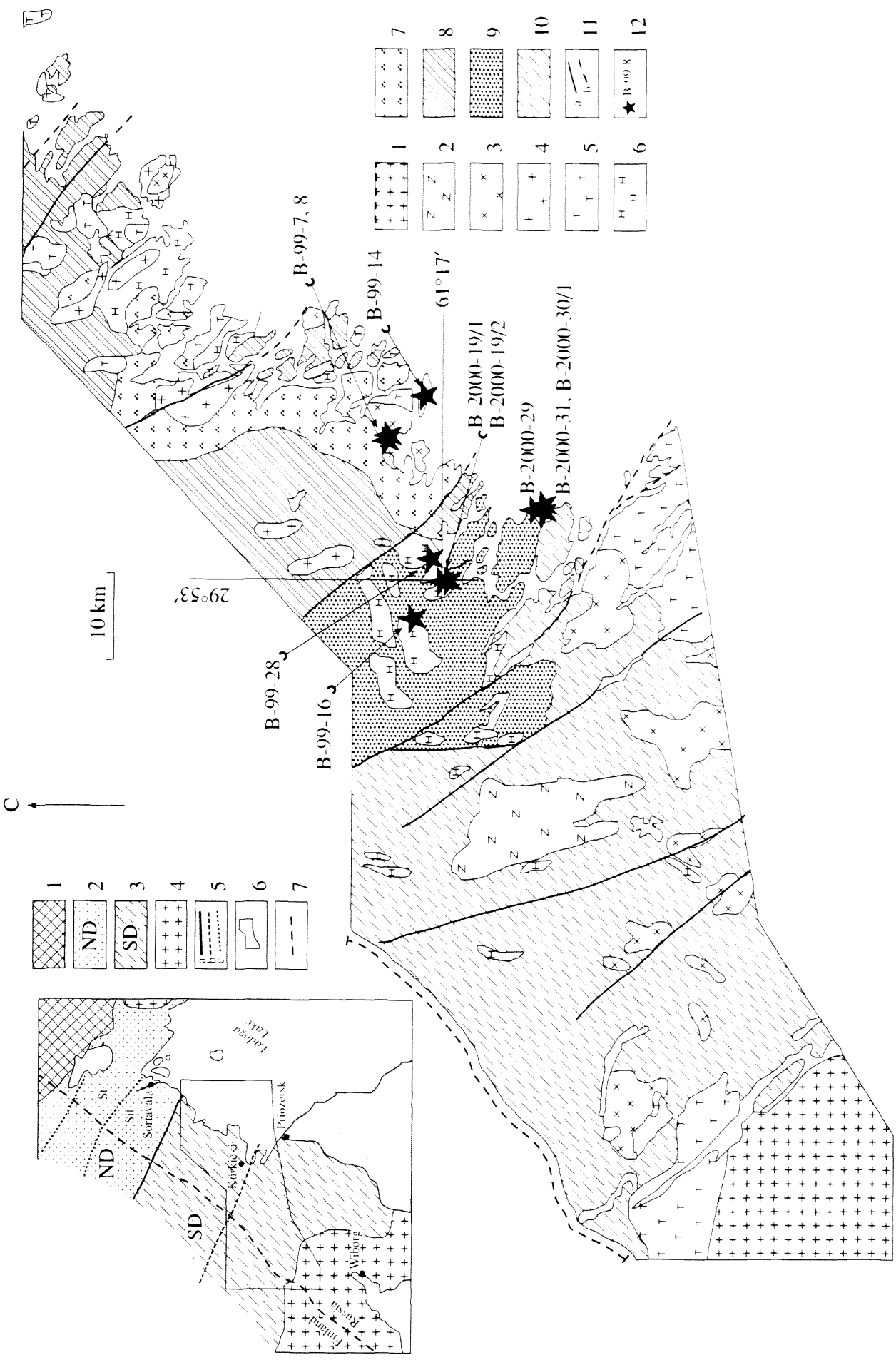

Fig. 1. Geological map of the southern domain and sampling sites.
(1) Early Riphean anorogenic rapakivi; (2–6) Svecofennian plutonic complexes: (2) postorogenic monzonites and granites, (3) late-orogenic granites, (4–6) synorogenic intrusions (4—tonalites, 5—diorites, 6—enderbites); (7–10) Early Proterozoic metamorphic gneisses: (7) predominantly biotite gneisses, (8) biotite–garnet gneisses, (9) hypersthene–garnet gneisses, (10) cordierite–sillimanite–garnet gneisses; (11) faults: (a) traced, (b) inferred; (12) sampling sites and sample numbers.
Inset: (1) Archean craton; (2, 3) Late Paleoproterozoic (Svecofennian) metamorphic complex: (2) Northern Domain (ND), (3) Southern Domain (SD); (4) rapakivi; (5a) offset plane of the overthrust separating the Northern and Southern domains, (5b) boundary between the Lahdenpohja and Priozersk subzones, (5c) boundaries between zones with different metamorphic grades; (6) study area; (7) state boundary. Shaded fields correspond to continental areas with Riphean deposits.

nics. The Priozersk zone is devoid of high-Ca rocks and consists mostly of metapelites and moderately aluminous metasiltstones with a pronounced potassic tendency. The rocks of both zones are extensively migmatized, with the Lahdenpohja zone containing predominantly sodic migmatites, while migmatites in the Proizersk zone being exclusively potassic. Provinces of sodic and potassic migmatites were also recognized on the regional scale in the Svecofennides (Ehlers *et al.*, 1993). Both migmatite zones underwent a complicated succession of deformations, which resulted in systems of strongly compressed northerly and northwesterly folds of different orders, whose hinges plunge to the south-southeast.

The zoning in the SD is manifested in the development of intrusions. The early- and synorogenic I-type intrusions consist of norite–enderbite and gabbro–diorite–tonalite complexes and are mostly restricted to the Lahdenpohja zone. The syn-, late-, and postorogenic intrusions of S-type potassic granites are widespread in the Priozersk zone, where they form relatively large plutons.

MAJOR STAGES OF ENDOGENIC ACTIVITY

Several Soviet, Russian and foreign researchers conducted long-term studies of the area with the aim of distinguishing the main stages during which the magmatic and supracrustal Svecofennian rocks had been produced. As a result, the age of active Svecofennian orogenic processes was constrained within the time span of 2.2–1.8 Ga (Tugarinov and Bibikova, 1980; Korsman *et al.*, 1988; and others).

The oldest constituents (1970 Ma) of the Svecofennian orogen are the Jormua ophiolitic associations (Gaal and Gorbatschev, 1987; Pekkarinen and Lukkarinen, 1991). The final rifting stages were responsible for the development of young (1970–1920 Ma) island arcs (Ekdahl, 1993) and the accumulation of deposits in the related forearc and backarc basins.

The ZMC is composed mostly of Early Proterozoic volcano-sedimentary rocks. Analogous sequences are widespread in Finland, where the volcanics in the Tampere schist belt (in southern Finland) were dated from 1904 ± 4 to 1889 ± 5 Ma (Simonen, 1980; Kahkonen *et al.*, 1989; Lahtinen, 1994). Considering that the youngest zircon age of the turbidites is equal to 1.91 Ga (Huhma, 1991), the accumulation of the Svecofennian turbidites can be dated at a narrow time interval of 1.91–1.89 Ga (Kahkonen *et al.*, 1989; Shul'diner *et al.*, 2000). The age of the Ladoga (corresponding to the Ludicovian) volcanic sequences was determined as 1.99–1.96 Ga (Baltybaev *et al.*, 2000).

The ultrametamorphic events in Svecofennian rocks exposed in parts of Finland adjacent to the Ladoga area were dated at 1.88 Ga for the plagiomigmatites near Turku (Mouri *et al.*, 1999) and at 1.80–1.82 Ga for rocks in the southern Finland zone of potassic granites and migmatites (Vaisanen *et al.*, 2002).

A broad spectrum of intrusive rocks in the Ladoga area yielded ages from 1.89 to 1.80 Ga for the early-, syn-, late- and postorogenic granitoids (Pushkarev and Ryungenen, 1995; Ivanikov *et al.*, 1996; Konopelko *et al.*, 1998; Bogachev *et al.*, 1999; Shul'diner *et al.*, 2000). The cratonization of the area ended with the emplacement of large rapakivi plutons. The oldest of them, the Wiborg Massif, was dated at 1646–1630 Ma (Vaasjoki and Rämö, 1989).

METAMORPHIC ROCKS AND MIGMATITES

Metamorphic and magmatic processes in the high-grade metamorphic zone occurred in a number of stages and produces corresponding rock associations. The most widespread high-temperature metamorphic rocks are variably migmatized aluminous garnet-bearing rocks. The metamorphic stages recognized in them gave rise to the following major mineral assemblages.

The **early stage** is characterized by granulite-facies mineral assemblages: *Opx+Cpx* ± *Grt* + *Hbl* + *Pl* ± *Qtz*, *Grt* + *Opx* + *Bt* + *Pl* ± *Kfs* + *Qtz*, and *Grt* + *Crd* ± *Sil* + *Bt* + *Pl* ± *Kfs* ± *Qtz*(±*Spl*).[1] The ore minerals are usually ilmenite, magnetite, and sulfides (the cordierite paragneisses sometimes contain sphalerite). The rocks are moderately migmatized.

The **intermediate stage** produced amphibolite-facies assemblages, overprinted on the earlier high-temperature mineral assemblages: *Grt* + *Cum* + *Cpx* + *Pl*, *Hbl* + *Pl* + *Qtz*, *Grt* + *Bt* + *Pl* ± *Kfs* + *Qtz*, and *Grt* + *Crd* ± *Sil* + *Bt* + *Pl* ± *Kfs* ± *Qtz*. The rocks are extensively migmatized.

The **late-stage** metamorphism resulted in relatively low-temperature alterations under andalusite–muscovite subfacies conditions. The retrograde alterations were particularly intense in the junction zone of the two domains. The aforementioned mineral assemblages are supplemented with muscovite, andalusite, Mn-bearing garnet, and, sometimes, chlorite.

The rock samples selected for geochronologic purposes represented all major types of the metamorphic rocks with high-temperature mineral assemblages. These were garnet–hypersthene and garnet–cordierite gneisses (B-2000-19/1 and B-99-16) from the Lahdenpohja subzone and a garnet–cordierite–sillimanite gneiss from the Priozersk subzone (B-2000-31). The compositions of these rocks are characterized in Table 1.

Taking into account that rocks in the Ladoga area were migmatized in a number of stages (Sudovikov,

[1] Mineral symbols: *Ab*—albite, *An*—anorthite, *And*—andalusite, *Ap*—apatite, *Bt*—biotite, *Chl*—chlorite, *Cpx*—clinopyroxene, *Crd*—cordierite, *Cum*—cummingtonite, *Fsp*—feldspar, *Grt*—garnet, *Hbl*—hornblende, *Ilm*—ilmenite, *Kfs*—potassic feldspar, *Ky*—kyanite, *Ms*—muscovite, *Mag*—magnetite, *Mnz*—monazite, *Opx*—orthopyroxene, *Pl*—plagioclase, *Qtz*—quartz, *Sil*—sillimanite, *Spl*—spinel, *St*—staurolite, *Zrn*—zircon, *r*—ore mineral(s).

Table 1. Mineralogical composition of samples used for isotopic dating

Minerals			Silicates									Other						Secondary	
no.	Sample	Rock	*Grt*	*Crd*	*Sil*	*Bt*	*Opx*	*Hbl*	*Kfs*	*Pl*	*Qtz*	*Ap*	*r*	*Ilm*	*Zrn*	*Mnz*	*Mag*	*Ms*	*Chl*
Intrusive rocks																			
1	B-99-7	Tervu granite				+			+	+	+	+			+			+	+
2	B-99-8	Tervu aplite				+		±	+	+	+		+			+		+	+
3	B-2000-29	Kilpola granite	+			+			+	+	+				+	+			
4	B-99-14	Lauvatsaari diorite	±			+		+	±	+	+	+	+		+				
5	B-99-28	Kurieki enderbite	±			+	+	+		+	+	+	+	+	+		+		
Metamorphic rocks and migmatites																			
6	B-99-16	*Grt-Crd-Bt* gneiss	+	+		+			±	+	+	+				+			
7	B-2000-31	*Grt-Crd-Sil* gneiss	+	+	+	+			+	+	+		+			+			
8	B-2000-19/1	*Opx-Grt* gneiss	+			+	+		+	+	+	+	+		+	+			
9	B-2000-19/2	leucosome II	+			+			+	+	+				+	+			
10	B-2000-30/1	leucosome II	+			+			+	+	+				+	+			

1955; Saranchina, 1972; Sedova *et al.*, 1989; and others), it was difficult to select a rock suitable for migmatite dating. It is pertinent to add that the studies conducted mostly by Scandinavian geologists in the early 1990s in the southern part of the Baltic Shield (Korsman *et al.*, 1988, Ehlers *et al.*, 1993) led them to a concept of two high-temperature stages of metamorphism and migmatization in the geologic history of the Svecofennides. These authors believed that the provinces of potassic and sodic migmatites recognized in the Svecofennides (and traced into the Ladoga area) have ages of 1.81–1.84 and 1.87–1.89 Ga, respectively. Proceeding from these data and considerations, we conducted our geochronologic research on two most typical migmatite types, which belong to two compositionally distinct migmatization zones.

The leucosome of the migmatites from the sodic province (sample B-2000-19/2 from the vicinity of the settlement of Kurkieki) developed in metaturbidites (sample B-2000-19/1). Metaturbidites of this type are widespread near the town of Lahdenpohja and the settlement of Kurkieki. These rocks are mostly hypersthene–garnet–biotite plagiogneisses alternating with garnet–biotite and hypersthene–biotite plagiogneisses. The sequences typically consist of cyclically intercalating thin layers of these gneiss types. Elsewhere hypersthene gneisses can occur as relatively thick (from tens to hundreds of meters) layers.

The leucosome of migmatites in the potassic province (sample B-2000-30/1, Kilpola Island) developed in aluminous (garnet and cordierite–sillimanite) gneisses (sample B-2000-31). Cordierite gneisses are widespread in the southern part of the ZMC (potassic province, Priozersk zone), where garnet–biotite and other gneisses occur in subordinate amounts. These gneisses mostly have a two-feldspar composition with variable proportions of cordierite, garnet, sillimanite, and biotite.

The leucosomes in the plagiogneisses have compositions basically different from those of leucosomes in the aluminous gneisses: the leucosomes are plagiogranitic in the former and are closer to potassic granites in the latter. The compositions of the rocks are characterized in Table 1.

The relationships between these leucosomes and other migmatite veins observed in outcrops led us to assign the leucosomes to the second generation in the genetic sequence. Morphologically, these leucosomes are veins 10–15 cm thick, which are folded into isoclinal folds conformably with the host gneisses.

INTRUSIVE ROCKS

Within the granulite part of the ZMC, magmatic rocks are grouped in three major complexes: Kurkieki, Lauvatsaari–Impiniemi, and Tervu (Shul'diner *et al.*, 1996). This succession of magmatic complexes was produced during the main stage of plutono-metamorphic activity in the Ladoga area, which included two stages of Svecofenian deformations: early orogenic (compressed isoclinal subvertical folds; the Kurkieki and Lauvatsaari–Impiniemi complexes) and late orogenic (overprinted faults and the Tervu Complex). This subdivision is clearly correlated with changes in the mineral assemblages of the metamorphic rocks and in the character and style of migmatization (there are obvious correlations between the metamorphic mineral transformations and the development of certain types of magmatic rocks). Late in the intermediate metamorphic stage, relatively rare potassic garnet-bearing granodiorites and granites were emplaced, which are specific of the Ladoga area and are considered independently of the aforementioned schemes. This type of granites was

provisionally recognized as a complex of garnet-bearing granites of Kilpola type.

Kurkieki Complex. This complex is dominated by enderbites and contains volumetrically subordinate norites and gabbronorites. The major rock-forming minerals of the enderbites are hypersthene, biotite, plagioclase, and quartz; some varieties additionally contain garnet, amphibole, clinopyroxene, and, very rarely, potassic feldspar. The accessory minerals are apatite, magnetite, graphite, zircon, and rutile. Ultramafic rocks are rare and occur as pyroxenite and cortlandite xenoliths in the enderbites. In the Ladoga area, enderbites are spread most widely within two sites: Kurkieki and Lahdenpohja, where they are closely associated with hypersthene-bearing gneisses. The restriction of the enderbites to granulite-facies metamorphic zones was noted by many researchers (Korsman *et al.*, 1984; Shul'diner *et al.*, 1997b). The enderbites themselves also show traces of high-temperature metamorphism in the form of recrystallization of all minerals, including hypersthene. Sample B-99-28, which was used in our geochronologic research, was taken from the Kurkieki enderbite site within the Kurkieki intrusion (Fig. 1).

Lauvatsaari–Impiniemi Complex. The complex consists of successively emplaced gabbro, diorite, and tonalite phases. These rocks are made up of hornblende, clinopyroxene, biotite, plagioclase, garnet, and quartz, whose amounts can vary from rock to rock. The accessory minerals are apatite, zircon, ilmenite, and magnetite. The rocks are often gneissose and have granoblastic textures. The rocks of the Lauvatsaari–Impiniemi Complex are known to often intersect enderbites, gneisses, and migmatites metamorphosed to the granulite facies. Both the geological relationships between and the mineral assemblages of these rocks suggest that they were produced after the metamorphic culmination, under amphibolite-facies metamorphic conditions. Sample B-99-14 was taken in Lauvatsaari Island, from the so-called Lauvatsaari diorite intrusion (Fig. 1).

Complex of garnet-bearing granites (Kilpola type). The main rock type of this complex is garnet leucogranites. These rocks occur in relatively minor amounts in Kilpola and Vavasari islands. It was determined that the Vavasari granites are crosscut by metadiorite dikes. A distinctive feature of the leucogranites is their high K-feldspar contents at very insignificant amounts of biotite and 15–20% garnet. According to their composition, these granites were classed with type S, which is produced by anatexis under high-grade metamorphic conditions. The granites are in places strongly gneissose and have granoblastic textures. The rock-forming minerals of both the Kilpola and the Vavasari granites are rich in optically discernible fluid inclusions. Sample B-2000-29 was taken in the northeastern tip of Kilpola Island (Fig. 1).

Tervu Complex. The predominant rock variety of this complex is two-feldspar granite. Along with potassic feldspar and plagioclase, the rocks contain biotite and quartz. The accessories are apatite, zircon, ilmenite, and magnetite. The granites sometimes contain secondary muscovite. The rocks are sometimes weakly gneissose. Sample B-99-7 was taken within the central part of the Tervu pluton (Fig. 1).

The pluton is cut by aplite veins, which crystallized late during the development of the Tervu Complex. The mineralogic composition of these veins is close to the composition of the rocks that make up the pluton itself. To date the youngest plutono-metamorphic events, we took sample B-99-8 from one of these aplite veins in the central part of the Tervu pluton (Fig. 1).

The composition of the magmatic rocks is characterized in Table 1.

METAMORPHIC MINERALS AND MINERALOGICAL CHRONOMETERS

Garnet. This mineral is usually randomly distributed in the metamorphic rocks. It was noted to occur only in some of the successively developing generations of the leucosome. Garnet is widespread in the tonalites but is much less typical of the basic and acid varieties of the metaintrusive rocks. This mineral practically never occurs as euhedral crystals, except only for the spessartine-rich garnet in young migmatite-granite veins. Garnet in the aluminous rocks often exhibits helicitic textures with finely acicular sillimanite. Garnet in the high-temperature part of the ZMC shows reversed chemical zoning, with the Mg mole fraction decreasing rimward. Zoning of this type is typical of garnet in both metamorphic and magmatic rocks. The only exception is the unzoned spessartine-rich garnet in the late migmatite–granite veins. The garnet is often replaced by biotite, plagioclase, and cordierite.

Cordierite. This mineral occurs as porphyroblasts or reaction rims around garnet and is typical of the aluminous gneisses. The cores of cordierite grains often contain helicitic sillimanite. The chemical zoning of the cordierite is weak, with the Mg mole fraction increasing from the cores to rims. Some cordierite grains contain spinel, zircon, and monazite, The cordierite is often replaced by biotite and an unidentified optically isotropic mineral.

Sillimanite. Sillimanite often occurs as inclusions in garnet and cordierite from the aluminous gneisses. The matrix of these gneisses sometimes contains larger sillimanite crystals.

Hypersthene. This mineral is contained mostly in rocks devoid of potassic feldspar (enderbites and mafic granulites). Hypersthene grains show weak chemical zoning, which depends on the neighboring minerals. This mineral is most typically replaced by biotite, cummingtonite, or hornblende.

Biotite. Biotite is the most widespread mineral of the rocks and is contained in virtually all of their types, in which it occurs in several generations. The younger biotite is usually relatively low in K (to 0.7 f.u.). The

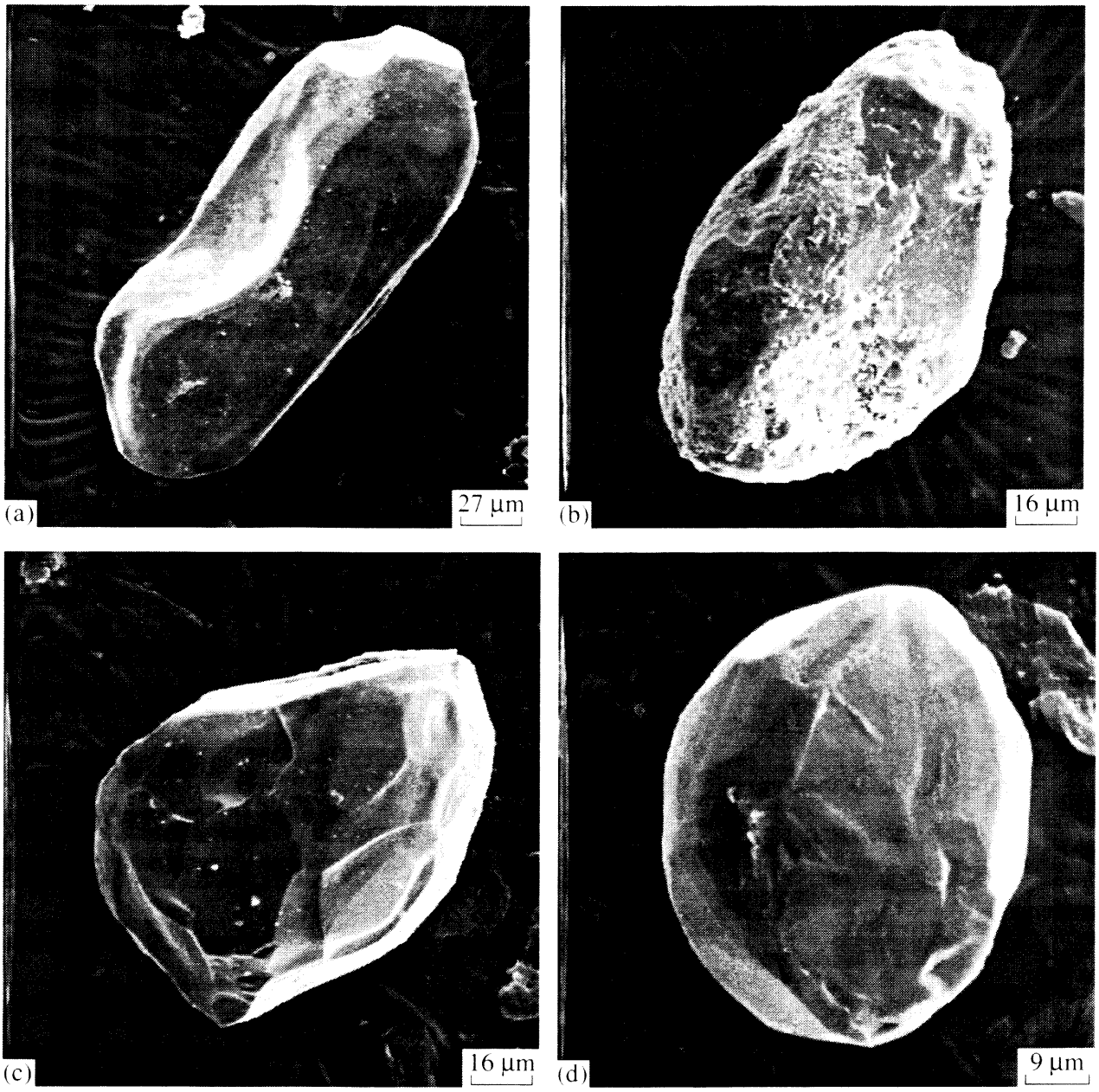

Fig. 2. Back-scattered electron images of monazites.

Monazites: (a) from granites (sample B-2000-29); (b) from an aplite vein (sample B-99-8); (c) from aluminous gneiss (sample B-2000-31); (d) from hypersthene–garnet gneiss (sample B-2000-19/1).

secondary biotite replaces garnet (often together with plagioclase). The biotite is, in turn, sometimes replaced by chlorite, hydromicas, and, rarely, andalusite.

Amphibole. The garnet-bearing rocks commonly contain columnar or stringy cummingtonite, which develops after hypersthene. Hornblende is characteristic of the magmatic rocks (diorites and tonalites). The amphibole of the altered rocks is replaced by biotite and chlorite.

Plagioclase. This mineral occurs in all rock types. The Ca mole fraction of the plagioclase depends on the bulk rock composition and corresponds to 20–30% *An* in the aluminous rocks and 30–40% *An* and higher in the garnet–biotite and garnet–hypersthene gneisses. The composition of the plagioclase usually varies very insignificantly within a petrographic thin section. The mineral is replaced by sericite (muscovite) and quartz.

Potassic feldspar. The mineral occurs in the aluminous gneisses in the form of large porphyroblasts of grid-twinned microcline in the leucosome. Some of the garnet–hypersthene gneisses contain high-temperature orthoclase-perthite. The mineral is widespread in the intermediate and acid intrusive rocks but is very scarce in the enderbites, in which it occurs as an interstitial mineral. The potassic feldspar is typically replaced by muscovite, quartz, and, sometimes, sillimanite (fibrolite).

Monazite. The principal morphological characteristics of the monazite are illustrated in Fig. 2. The analysis of the morphometric and geochemical features of monazite crystals led us to subdivide them into two groups.

Group 1 comprises monazite crystals from intrusive rocks (samples B-99-8, B-2000-29, and 115). These are subhedral prismatic crystals or angular grains. The monazite from our samples consists mostly of yellow turbid grains >100 μm in size. The surface of these grains is in places porous, with small overgrowths (Figs. 2a, 2b). The surface alterations of these crystals were, perhaps, caused by postmagmatic processes. The Th/U ratios of the monazite of this group are at a maximum and vary from 11.9 to 22.6, the U content is 1120–2590 ppm.

Group 2 consists of monazite from the metamorphic rocks, gneisses, and leucosomes (samples B-2000-19/1, B-2000-19/2, B-2000-31, B-2000-30/1, and B-99-16). The metamorphic rocks contain predominantly equant and rounded pale yellow transparent monazite grains, which are more euhedral than the group-1 crystals (Figs. 2c, 2d). The size of pale yellow monazite grains from the gneisses is 30–75 μm, and these grains from the leucosomes are 50–200 μm. In addition, the aluminous gneisses and their leucosome (samples B-2000-31, B-2000-30/1, and B-99-16) contain relict monazite in the form of prismatic yellow crystals that compose the cores of pale yellow monazite grains. The U/Pb age of each sample was estimated using pale yellow transparent crystals. Because of the low monazite contents in some of the samples, the proportions of relict and pale yellow transparent crystals in the analyzed monazite batches could significantly vary. All group-2 monazites had low Th/U ratios, from 7.5 to 13.5, at U contents from 530 to 1010 ppm. The exception is sample B-2000-31 (Table 2).

The equant monazite with low Th/U ratios (<14) found in Svecofennian rocks from Finland (Mouri *et al.*, 1999) and amphibolite-facies paragneisses (Fostre *et al.*, 2002) were ascribed to metamorphic minerals. Because of this and taking into account the relation of the group-2 monazite to metamorphic rocks and their morphological and geochemical characteristics, we believe that this type of monazite is metamorphic.

Zircon. Zircon was examined in the intrusive rocks and the leucosomes of the migmatites, for which the simultaneous occurrence of grains of different origin is less probable. We did not study this mineral from the gneisses, because, according to our observations and literature data (Tugarinov and Bibikova, 1980; Huhma *et al.*, 1991), these rocks may contain zircon of different genesis and age. Note that we also found older detrital zircon in the leucosomes of the migmatites (sample B-2000-30/1). The morphology of the zircon and its inner structure are illustrated (as is seen in transmitted light, cathodoluminescence, and BSE) in Figs. 3a–3f. Zircon from our samples is characterized below.

Sample B-99-28: enderbite. This rocks is dominated by long-prismatic subhedral zircon crystals of yellow–brown and pale yellow color or colorless, with traces of secondary growth, dissolution, and deformations. The rock also contains moderately prismatic and short-prismatic varieties and parallel aggregates of crystals, suggesting that this zircon crystallized from a melt. The length l of the long-prismatic crystals is 30–700 μm at an elongation coefficient of $4 < K_e < 9$. The moderately prismatic grains have $1.8 < K_e < 3.3$ at $l = 250$ μm. It can be seen under the microscope that the zircon grains are zoned, have a blocked inner structure, and are strongly fractured (more than ten fractures per grain). Dark and pale crystals have brown rims (pale crystals have thinner rims). The BSE images of the zircon show that fractures in these crystals are marked by halos, which have a clearly different age. As was demonstrated by Hanchar and Miller (1993), a paler color in grain margins corresponds to elevated concentrations of Hf, Y, and U. Occasional grains are weakly zonal, and no more than one-third of all crystals is optically homogeneous. The U concentration in the brown crystals varies from 690 to 2140 ppm, these values for the pale crystals are 1220–1520 ppm, and the Th/U ratios are 0.14–0.22, with lower values typical of the brown grains. It should be mentioned that Th/U ratios from 0.2 to 0.4 (Fig. 4) are typical of altered magmatic zircon grains (Schaltegger *et al.*, 1999). Literature data and our observations indicate that the Th/U ratio of magmatic zircon can vary within broader limits and is rather controlled by the rock chemistry, geodynamic environment (Bibikova, 1989), or the regional geochemical features of the rocks. For example, the Th/U ratio of zircon in enderbites from the Aldan Shield is ~0.6–0.7 (Berezhnaya, 1999). After the etching of polished zircon sections with HF vapor, it can be clearly seen that these crystals consist of two types of material with different metamictness. The more metamict phase may be present in both the peripheral and central portions of the crystals.

It is interesting to compare the morphological parameters of zircon from sample B-99-28 and from the enderbites of the Kurkieki intrusion (sample 105; Kotov *et al.*, 1992). Zircon crystals in these samples are generally similar, but the zircon of sample 105 is more euhedral, devoid of brown crystals, has a low U content (U < 400 ppm), and yields an older age. The comparison of the main characteristics of zircon from these samples led us to conclude that sample B-99-28 represents an enderbite variety produced during a later evolutionary stage of the massif, because its zircon is strongly enriched in U and, perhaps, also Th. The brown rims of zircon grains from the enderbites likely grew during younger processes (chemically, the brown zircon is the closest to the zircon from leucosome II in the garnet–hypersthene gneisses).

The pale brown zircon contains rare fluid inclusions. The most transparent central portion of a zircon grain contain an inclusion with a gas phase. Fractures running across the elongation of the grain host planar inclusions, which seem to trail subparallel zones of healed fractures. Groups of gas–liquid inclusions were detected in the newly-formed rims overgrowing zircon grains. These inclusions are sometimes two- and even three-phase

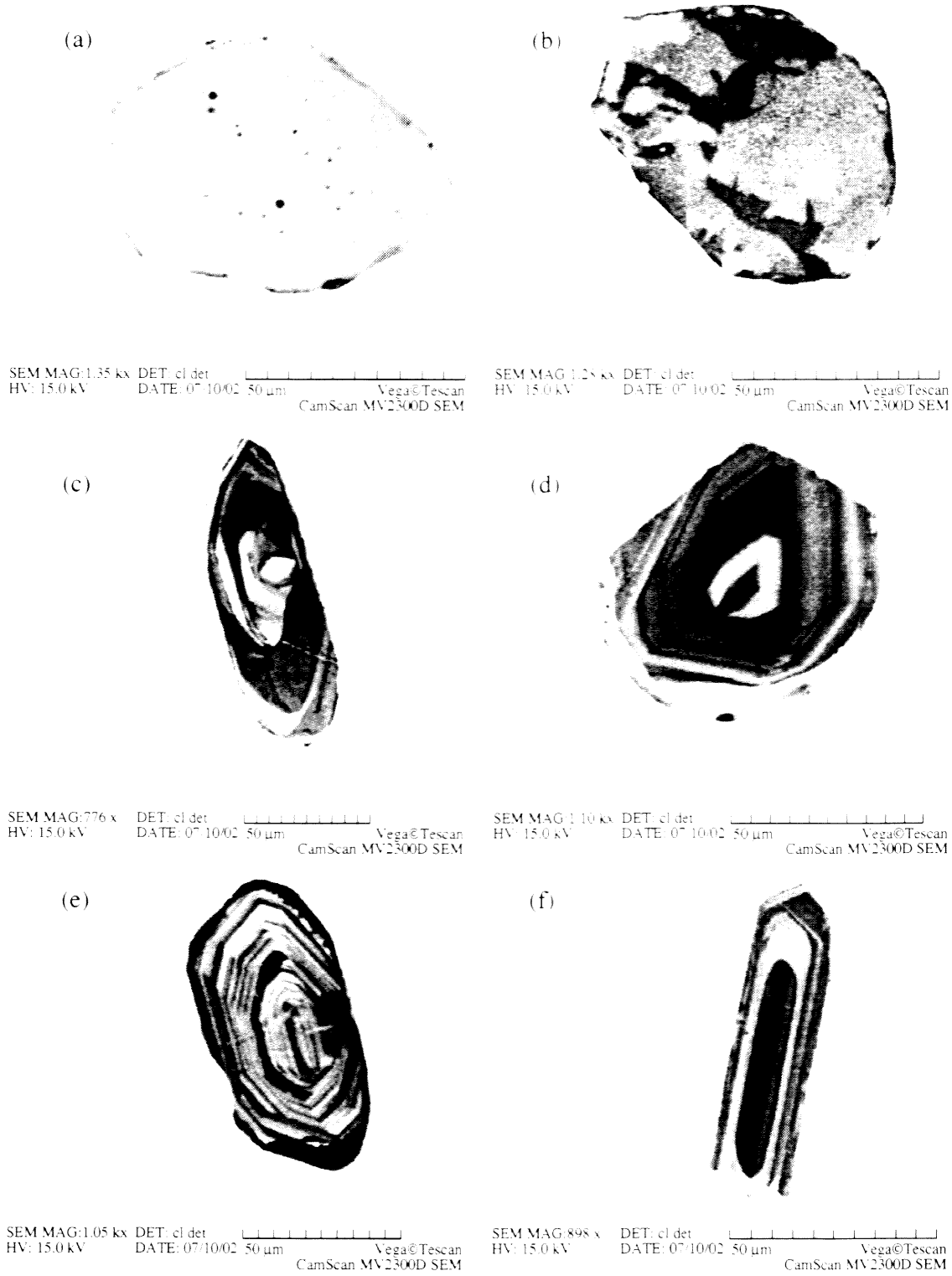

Fig. 3. Cathodoluminescence images of zircon from the leucosome of garnet–orthopyroxene gneiss (sample B-2000-19/2). (a–d) Predominant (80%) pale pink and brown subhedral equant zircon grains (type I), consisting of detrital cores and thick zonal rims; (e–f) pale pink and brown subhedral long-prismatic zircon grains (type II) with thin rims of variable thickness.

($L + G + G$ and $L + L + G$).[2] Observations suggest that the inclusions are of two types of: (i) single larger inclusions not restricted to fractures and containing a gas phase and (ii) smaller inclusions spatially restricted to fractures and cracks and occurring as groups of 3–7 inclusions.

It can be concluded that zircons from the Kurkieki enderbites show evidence of their magmatic and metamorphic genesis and were formed by the reworking of magmatic zircon by a high-temperature metamorphic fluid.

Sample B-99-14: diorite. Zircon from this diorite is more euhedral than from the enderbites. The zircon grains are prismatic to long-prismatic, have a hyacinth habit, are pale, have high birefringence, and magmatic-type zoning. The length of the crystals is $40 < l < 450$ µm at $2 < K_e < 7$. Their BSE images show weak

[2] *L*—liquid, *G*—gas.

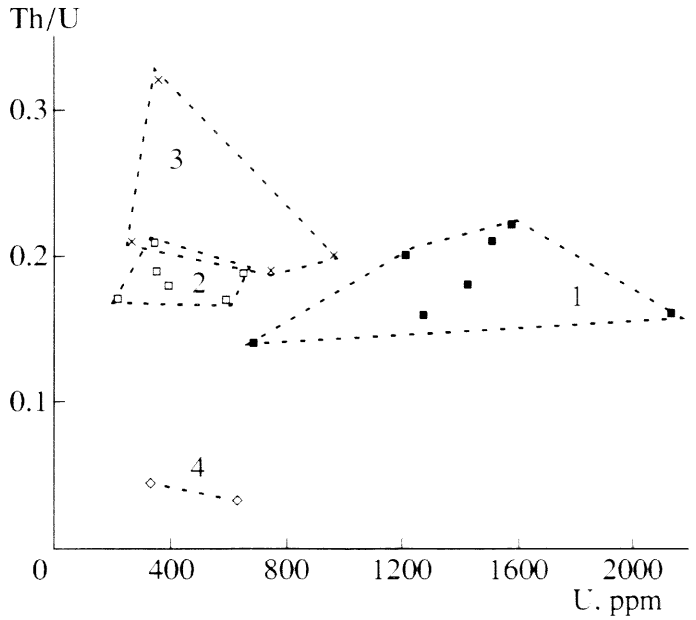

Fig. 4. Th/U ratios of zircon from magmatic rocks and migmatites. (1) Enderbite (B-99-28); (2) diorite (B-99-14); (3) granite (B-99-7); (4) migmatite (B-2000-19/2 and B-2000-30/1).

zoning with slight alterations in the margins and along fractures; some crystals are homogeneous. The U concentrations are 220–660 ppm, and the Th/U ratio varies very insignificantly: from 0.16 to 0.21. The zircon contains numerous elongated mineral inclusions (which are often oriented across the elongation of the host zircon grains), and ~20% of the grains bear fluid inclusions (which are very small). There seems to be no order in the distribution of these fluid inclusions. The zircon grains are relatively insignificantly fractured (~10–15% grains), with up to 3–4 fractures per grain. Fractured grains are commonly richer in fluid inclusions.

Judging from their morphology, zircon from the diorites are magmatic, with pronounced postmagmatic or metamorphic alterations.

Sample B-99-7: granite. The granite contains two zircon varieties. One of them comprises transparent pink short-prismatic subhedral zoned crystals, which are 30–200 μm long and have $1.3 < K_e < 2.0$. The other, predominant, variety consists of prismatic and long-prismatic turbid pinkish yellow zircon grains with coarse zoning. The crystals are 40–300 μm long, with $2 < K_e < 4$. In BSE images, zircon grains of both varieties are homogeneous grains with weak alterations in the margins. The U contents vary from 370 to 970 ppm at $0.19 < \text{Th/U} < 0.32$.

Approximately one-third of the grains (60–80 grains from this selection) contains fluid inclusions, which are slightly more abundant in dark-colored zircon crystals. The inclusions are single or occur as groups of up to 5–6 planar inclusions. No phases are discernible in them. Some grains also contain rounded solid and, sometimes, acicular inclusions, as long as ~1/5 of the length of the host zircon crystal. Inclusions are often restricted to one or two growth zones of zircon grains, some grains abound in inclusions in the marginal zones. The zircons are notably fractured, from 1–2 to 5–6 fractures per grain.

According to their morphology and the low U contents, the group-1 zircons were ascribed to the early magmatic type, while the group-2 grains seem to be late-magmatic zircons.

Sample B-2000-19/2: leucosome of migmatite in garnet–hypersthene gneiss. The leucosome of the *Opx-Grt* gneisses is dominated (80%) by pale pink and brown subhedral equant zircons (type I), which consist of detrital cores and zonal rims. The elongation coefficient of the crystals K_e ranges from 1 to 2.2, and their length is 60–300 μm. Approximately 20% of the selected grains consists of pale pink and brown zircon crystals (type II). They are long-prismatic, subhedral, zonal, with thin unequal rims. The crystals are 50–425 μm long at $3 < K_e < 8.5$. The selection includes numerous aggregates of two to three individuals. Although the grains are extensively fractured (>10 fractures per grain), they remain transparent. Fluid inclusions are rare and are mostly concentrated within crystal cores. Some crystals contain two-phase inclusions, which are readily visible in transmitted light. This type of zircon is characterized by low Th/U ratios of 0.03–0.04 at U contents from 330 to 620 ppm. Th/U ratios greater than 0.2 are usually thought to be typical of zircons from leucosome (Mouri *et al.*, 1999; Schaltegger *et al.*, 1999) and are reportedly explained by the concurrent crystallization of zircon and monazite (Moeller, 2001). This led us to hypothesize that the metamorphic monazite had crystallized somewhat earlier than the zircon and, consequently, the bulk of Th from the melt had been accommodated in the monazite.

For the U–Pb dating of zircon, we used grains of type II, whose geochemical and morphological characteristics allow their ascribing to the ultrametamorphogenic type.

Sample B-2000-30/1: leucosome of migmatite in garnet–cordierite–sillimanite gneiss. The sample contains two zircon types with strongly predominant zircon grains of type I. This type consists of small pink–cherry subhedral prismatic crystals and oval grains with traces of zoning. The crystals are 20–60 μm long at $1.5 < K_e < 2.0$. Cathodoluminescence shows that zircon of this type is strongly recrystallized and is, in fact, a new generation of this mineral. Type II of the zircons comprises colorless prismatic crystals, which are weakly zoned, transparent or turbid, with high birefringence. Cathodoluminescence of the type-II zircon reveals that its grains consist of cores and zonal rims. The crystals are 50–250 μm long and have an elongation coefficient of $2 < K_e < 3$. Judging from its morphology, this type of zircon is similar to zircon from the leucosome of the garnet–hypersthene gneisses (B-2000-19/2), which is ultrametamorphic, but these zircons contain relics of older detrital zircon.

Table 2. Results of the U–Pb isotopic study of zircon and monazite from rocks of the Ladoga area

No.	Size fraction (μm) and its characteristics	Sample, mg	Concentration, ppm		Isotopic ratios					Th/U (cryst.)	Rho	Age, Ma				
			Pb	U	$^{206}Pb/^{204}Pb^a$	$^{207}Pb/^{206}Pb^b$	$^{208}Pb/^{206}Pb^b$	$^{207}Pb/^{235}U$	$^{206}Pb/^{238}U$			$^{206}Pb/^{238}U$	$^{207}Pb/^{235}U$	$^{207}Pb/^{206}Pb$	concordant	proba-bility
B-99-28: enderbite, Kurkieki intrusion																
1	*Zrn*, >150, pale	0.57	500	1520	14090	0.11421	0.075154	5.067	0.3218	0.21	0.93	1798.4	1830.6	1867.4 ± 0.63	1881.4** (+9.3/–5.3)	0.94
2	*Zrn*, >150, pale, a.a.	0.39	540	1580	15930	0.11445	0.079755	5.227	0.3312	0.22	0.94	1844.4	1857.0	1871.2 ± 0.58		
3	*Zrn*, 70–80, pale	0.39	410	1220	16120	0.11444	0.071896	5.189	0.3289	0.20	0.94	1832.9	1850.8	1871.1 ± 0.58		
4	*Zrn*, >150, brown	0.78	220	690	9380	0.11412	0.050174	5.118	0.3253	0.14	0.90	1815.6	1839.2	1865.9 ± 0.76		
5	*Zrn*, >150, brown, a.a.	0.34	720	2140	13690	0.11449	0.059785	5.224	0.3309	0.16	0.94	1842.9	1856.6	1871.9 ± 0.56		
6	*Zrn*, 70–80, brown	0.30	430	1280	9480	0.11439	0.057498	5.181	0.3285	0.16	0.94	1831.1	1849.5	1870.3 ± 0.61		
7	*Zrn*, 100–150, brown, a.a.	0.36	490	1430	12770	0.11485	0.066138	5.309	0.3352	0.18	0.94	1863.7	1870.2	1877.5 ± 0.59		
B-99-14: diorite, Lauvatsaari intrusion																
8	*Zrn*, 100–150	0.64	180	590	3285	0.11532	0.062027	4.806	0.3022	0.17	0.94	1702.3	1785.9	1885.0 ± 0.60	1878.5** ±3.3	0.78
9	*Zrn*, 70–80	0.84	67	220	3185	0.11530	0.060987	4.746	0.2986	0.17	0.91	1684.2	1775.5	1884.5 ± 0.75		
10	*Zrn*, whole sample, a.a.	0.42	120	350	2168	0.11511	0.067665	5.100	0.3214	0.19	0.78	1796.4	1836.2	1881.6 ± 1.50		
11	*Zrn*, >100, a.a.	0.44	120	350	4848	0.11534	0.076831	5.118	0.3218	0.21	0.93	1798.6	1839.1	1885.2 ± 0.65		
12	*Zrn*, 80–100, a.a.	0.29	230	660	2913	0.11495	0.069109	5.295	0.3341	0.19	0.93	1858.2	1868.1	1879.1 ± 0.70		
13	*Zrn*, 80–100, a.a.	0.61	110	390	2602	0.11505	0.064215	4.180	0.2635	0.18	0.98	1507.6	1670.0	1880.7 ± 0.74		
B-2000-29: *Grt–Pl–Kfs* granite, Kilpola intrusion																
14	*Mnz*	n.a.	n.a.	n.a.	7263	0.11591	0.14852	6.7331	5.286	18.6	0.93	1868.1	1868.1	1865.0 ± 2.1	1866.9 ± 4.4	0.78

Table 2. (Contd.)

No.	Size fraction (μm) and its characteristics	Sample, mg	Concentration, ppm		Isotopic ratios					Th/U (cryst.)	Rho	Age, Ma				
			Pb	U	$^{206}Pb/^{204}Pb$[a]	$^{207}Pb/^{206}Pb$[b]	$^{208}Pb/^{206}Pb$[b]	$^{207}Pb/^{235}U$	$^{206}Pb/^{238}U$			$^{206}Pb/^{238}U$	$^{207}Pb/^{235}U$	$^{207}Pb/^{206}Pb$	concordant	probability
B-99-7: granite; Tervu intrusion																
15	*Zrn*, >100	0.35	97.0	370	918.7	0.11302	0.11710	3.681	0.2362	0.32	0.76	1367.1	1567.3	1848.6 ± 1.6	1860.8** ±2.6	0.89
16	*Zrn*, <70	0.36	200	740	3583	0.11325	0.069189	4.120	0.2638	0.19	0.88	1509.5	1658.3	1852.2 ± 0.87		
17	*Zrn*, >100, a.a.	0.33	75	260	2268	0.11529	0.075498	4.337	0.2728	0.21	0.98	1555.1	1700.4	1884.4 ± 0.88		
18	*Zrn*, <70, a.a.	0.37	300	970	10210	0.11401	0.071547	4.726	0.3006	0.20	0.94	1694.2	1771.7	1864.4 ± 0.59		
19	*Zrn*, yellow*	0.50	3800	2590	6995	0.11355	4.3164	4.874	0.3113	11.9	0.98	1747.1	1797.7	1857.0 ± 1.3		
B-99-8: vein granite, Tervu intrusion																
20	*Mnz*	0.20	2300	1120	2724	0.11774	5.9112	5.177	0.3329	16.4	0.92	1852.7	1848.8	1844.6 ± 2.1	1849.7 ± 4.4	0.44
B-2000-31: *Grt–Crd–Sil gneiss*																
21	*Mnz*	0.25	3140	1500	6139	0.11640	6.0920	5.256	0.3338	16.8	0.99	1856.9	1861.8	1867.3 ± 2.1	1860.5 ± 4.4	0.28
B-99-16: *Grt–Crd* gneiss																
22	*Mnz*	1.25	590	530	20580	0.11377	2.7053	5.184	0.3324	7.5	0.97	1850.0	1850.0	1850.0 ± 2.1	1850 ± 4.4	0.99
23	*Mnz*, a.a.	0.21	1710	1340	6145	0.11366	3.2811	5.257	0.3354	9.1	0.96	1864.7	1861.8	1858.7 ± 6.9	1862.4 ± 4.4	0.58
B-2000-19/1: *Grt–Opx* gneiss																
24	*Mnz*	0.26	4500	3020	24010	0.11492	3.9766	5.326	0.3378	11.0	0.95	1876.0	1873.0	1869.7 ± 2.1	1873.8 ± 4.4	0.52
B-2000-19/2: leucosome of generation-II migmatite																
25	*Mnz*	0.15	4590	4010	17750	0.11531	2.8132	5.317	0.3366	7.6	0.96	1870.5	1871.6	1872.9 ± 2.1	1871.3 ± 4.4	0.78
26	*Zrn*, >100	0.73	110	330	2092	0.12056	0.03278	5.149	0.3272	0.045	0.96	1825.0	1844.2	1866.0 ± 2.1		
27	*Zrn*, 60–85	0.40	200	620	3278	0.11855	0.022444	5.1167	0.3243	0.033	0.96	1810.7	1838.9	1871.0 ± 2.1		
B-2000-30/1: leucosome of generation-II migmatite																
28	*Mnz*	0.73	4880	3780	27620	0.11493	3.2999	5.342	0.3385	9.1	0.98	1879.5	1875.5	1871.2 ± 2.1	1876.5 ± 4.5	0.41
29	*Zrn*, <60 μm	n.a.	n.a.	n.a.	3690	0.11415	0.037313	5.140	0.3265	0.10	0.96	1821.6	1842.7	1866.6 ± 0.74		
30	*Zrn*, >100 μm	n.a.	n.a.	n.a.	2275	0.13194	0.14613	4.939	0.2715	0.40	0.92	1548.5	1809.0	2124.0 ± 1.6		

Note: [a] Isotopic ratios are corrected for the fractionation coefficient and blank; [b] isotopic ratios are corrected for the fractionation coefficient, blank, and common Pb; a.a.—air-abraded grains, * fraction 19 is a mixture of monazite and zircon. The blank was no higher than 0.1 ng for Pb and 0.01 ng for U. The Pb and U isotopic measurements were conducted on a MAT-261 mass spectrometer; the precision of individual U/Pb measurement was 0.50% (2σ), the precision of the $^{207}Pb/^{206}Pb$ ratio was 0.11% (2σ). All calculations were conducted by programs of Ludwig (1991, 1998). ** Concordant age by the upper intercept of the regression line and concordia. The Th/U ratios were calculated from the Pb isotopic age and the crystallization time of the mineral. The Pb and U isotopic measurements for the zircon fraction from sample 19 were carried out by L.A. Neymark (Institute of Precambrian Geology and Geochronology, Russian Academy of Sciences); n.a.—not analyzed.

The Th/U ratios of the zircon vary from 0.1 in type I to 0.4 in type II (Table 2). Zircon grains for dating were the clearest and purest grains of both types.

ISOTOPIC DATING

Metamorphic Rocks

Monazite from the garnet–hypersthene gneiss (sample B-2000-19/1) from the Lahdenpohja zone has a concordant age of 1873.8 ± 4.4 Ma (with a probability of 0.52 at 95% confidence level). The concordant age of monazite (with a probability of 0.28 at 95% confidence level) from sample B-2000-31 of the garnet–cordierite–sillimanite gneiss from the Priozersk zone is 1860.3 ± 4.4 Ma. The morphological analysis of the crystals allowed us to suggest that the monazite from sample B-2000-31 is recrystallized detrital monazite.

We have analyzed two monazite types from sample B-99-16. The predominant type I consists of pale yellow subhedral crystals with a low U content (530 ppm) and a younger age. The rock contains subordinate amounts of dark yellow subhedral monazite crystals (which possibly have cores) of older age. The sample of the garnet–cordierite–sillimanite gneiss (B-99-16) yielded a concordant monazite age of 1862.4 ± 4.4 Ma (with a probability of 0.58 at 95% confidence level) and an age of 1850 ± 4.4 Ma (with a probability of 0.99 at 95% confidence level). The low U concentrations in the monazite likely resulted from retrograde alterations, which could also reset the whole U–Pb system of this mineral.

Migmatites

The U–Pb age of ultrametamorphism was determined using monazite and zircon from the leucosome of migmatite of generation 2 (samples B-2000-19/2 and B-2000-30/1).

Zircon grains 60–85 μm in size from sample B-2000-19/2 (which is thought to have been affected by melting processes) are prismatic, zonal, and have a low Th/U ratio, i.e., show features typical of crystals growing from a melt (Rubatto *et al.*, 2001). They yielded an age of $t(^{207}Pb/^{206}Pb)$= 1871.1 ± 2.1 Ma (Table 2). This value coincides with the concordant age (with a probability of 0.78 at 95% confidence level) of monazite (1871.3 ± 4.4 Ma) from the same sample. Larger zircon grains are a little bit younger $t(^{207}Pb/^{206}Pb)$ = 1866.0 ± 2.1 Ma, perhaps, because the larger grains possess thin outer rims of a younger zircon generation (Fig. 3c).

At Th/U = 0.1, the age $t(^{207}Pb/^{206}Pb)$ = 1866.6 ± 0.74 Ma of zircon grains of the size fraction of <0.60 μm (sample B-2000-30/1) is younger than the concordant age of monazite from the same sample (1876.5 ± 4.5 Ma; Table 2, Fig. 5), perhaps, due to thin rims of newly formed zircon. At the same time, larger grains (>100 μm) give an age of $t(^{207}Pb/^{206}Pb)$ = 2124 ± 1.6 Ma. This fact suggests that the grains have inherited cores, which probably have a Proterozoic age.

Enderbites

The discordia defined by six (Table 2, nos. 2–7) of the seven points corresponding to the analyzed zircon fractions from the enderbites intercepts the concordia at two points: 1881.4 + 9.3/–5.3 and 630 ± 238 Ma, MSWD = 0.2. Point 1 was rejected because the zircon of this fraction had the most disturbed isotopic system. Given the magmatic genesis of the zircon, this age value was interpreted as the age of the enderbite (Table 2, Fig. 6a).

At the same time, the analysis of fluid inclusions in the zircon indicates that zircon from the Kurkieki enderbite is a mixture of magmatic and metamorphic phases, which were produced by the reworking of the magmatic zircon by a low-temperature metamorphic fluid. Inclusions of fluids of similar composition and density in rock-forming minerals from the high-temperature core of the ZMC were studied to constrain the granulite-facies metamorphic conditions, which were estimated at T = 815°C and P = 5.5 kbar (Baltybaev *et al.*, 2000). Thus, dating this enderbite, we also dated the granulite metamorphism of the Ladoga area at 1881.4 + 9.3/–5.3 Ma.

Diorites

Zircon grains contained in the diorite are more euhedral and less altered than in the enderbites. The lowest MSWD = 0.25 and age errors (1878.5 ± 3.3 Ma) were yielded by the discordia drawn through the four points of fractions 8–10 and 12 in Table 2. Point 13 was rejected because its zircon fraction had the most disturbed isotopic system. The age of 1878.5 ± 3.3 determined by the upper intercept with the concordia was assumed as the age of the diorite (Table 2, Fig. 6b).

Kilpola Granite

One of the massifs of these granites (sample B-2000-29), exposed north of Kilpola Island, yielded a monazite concordant age (with a probability of 0.78 at 95% confidence level) of 1866.9 ± 4.4 Ma (Table 2, Fig. 5).

Tervu Granites

Taking into account the relatively high age $t(^{207}Pb/^{206}Pb)$ of the abraded zircon grains (fractions 17 and 18 in Table 2), likely because of the presence of an old inherited radiogenic lead, we constructed an isochron on the basis of three points: the points of fractions 15, 16, and 19. The age corresponding to the upper intercept with the concordia was 1860.8 ± 2.6 Ma, MSWD = 0.007 and was interpreted as the age of the granite (Table 2, Fig. 6c). The concordant monazite age (with a probability of 0.44 at 95% confidence level) of the vein granite facies was determined as 1849.7 ± 4.4 Ma (Table 2, Fig. 5).

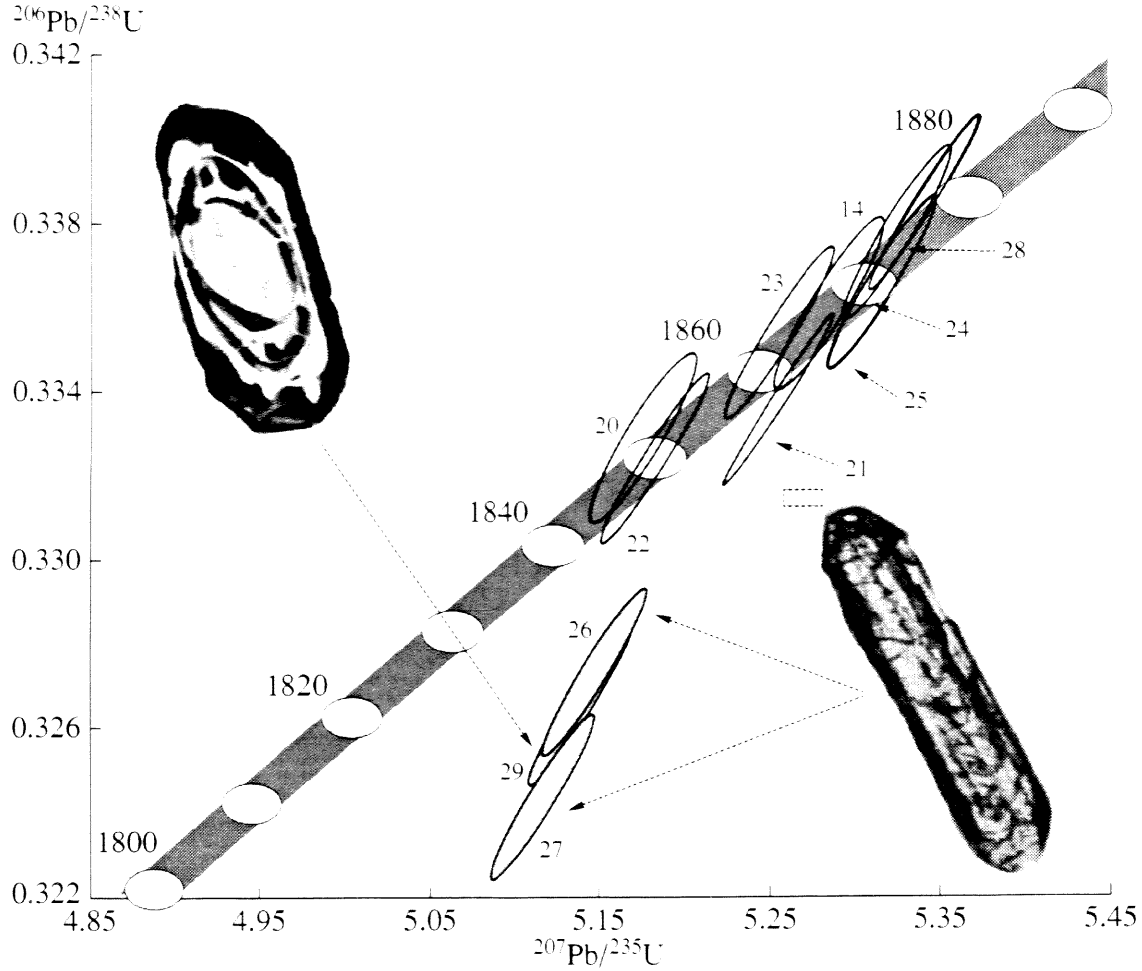

Fig. 5. Concordia plot for zircons and monazites (shaded ellipses and ellipses, respectively). Numerals near ellipses correspond to fraction numbers (see Table 2).

DISCUSSION

Metamorphic Rocks and Migmatites

The analysis of mineral assemblages in rocks from the southern (Priozersk) zone of the ZMC core and mineralogical thermometry of these rocks by the TWQ program with the use of the thermodynamic database for granulite assemblages (Berman, 1988, 1991; Berman and Aranovich, 1996) and by the THERMOCALC program (Powell and Holland, 1998) allowed us to constrain the granulite-facies metamorphic culmination parameters at T = 780–850°C and P = 5–6 kbar (Fig. 7).

The P–T parameters of the northern (Lahdenpohja) zone were evaluated earlier (Shul'diner *et al.*, 1997b). For the early stage, the *Grt-Crd* thermobarometer yielded T = 790–825°C and P = 5–5.8 kbar. The evaluations conducted using H_2O and CO_2 inclusions in granulite minerals yielded similar values: T = 815°C and P = 5.5 kbar. The metamorphic parameters of the intermediate stage were determined by the *Grt* and *Crd* compositions in reaction rims. These parameters were T = 820–590°C and P = 5.6–4.3 kbar. Fluid inclusions in minerals from the migmatites and magmatic rocks of this stage (diorites and tonalites) gave pressures from 6 to ~4 kbar. According to *Grt-Bt* thermometry, the late stage took place at T from 450 to 550°C and P = 2–4 kbar.

These evaluations, conducted using reactions with the participation of garnet and cordierite, led us to conclude that the P-T parameters of the metamorphic culmination in the Priozersk and Lahdenpohja migmatite zones were identical.

In spite of the high temperature values obtained for the Priozersk zone, orthopyroxene gneisses are generally atypical of it. Such gneisses could be expected to appear at temperatures of about 800°C and higher according to the reactions

$$Bt + Qtz = Opx + Kfs + H_2O$$

or

$$Bt + Grt + Qtz = Crd + Opx + Kfs + H_2O.$$

This seems to be explained by the high alumina contents of the rocks (they contain sillimanite), which limit the stability of hypersthene under pressures below 7 kbar according to the reaction

$$Opx + Sil + Qtz = Grt + Crd.$$

The occurrence of sillimanite during the metamorphic culmination is confirmed by Pb–Pb dating by means of stepwise sillimanite leaching from aluminous gneisses from the Priozersk zone (sample B-2000-31). It was

determined that the sillimanite had crystallized at 1880.1 ± 7.7 Ma (Baltybaev *et al.*, 2003).

The development of the Ladoga migmatites in a succession of stages is manifested in a number of leucosome generations that can be distinguished in some outcrops. The oldest thinly banded leucosome developed after *Opx–Cpx*, *Opx–Grt*, and *Grt–Crd–Sil* gneisses, whose temperatures were estimated at 800–850°C. This and the development of similar migmatites in enderbites, which were produced under granulite-facies conditions, provides grounds to believe that the early migmatites were related to the granulite metamorphism. The second-generation migmatites (whose isotopic age was also evaluated) were formed in relation with the development of diorite–tonalite massifs, which are younger than the granulites and related enderbites. The temperature interval of the second migmatization stage was estimated mostly by the *Grt–Crd* equilibrium. Petrographic observations indicate that the development of migmatites of this generation was coupled with the replacement of garnet by cordierite in the metamorphic rocks. The Fe–Mg distribution between the garnet and cordierite was utilized to evaluate the temperature range within which the migmatites had developed: it was from 800 to 600°C (Baltybaev *et al.*, 2000). The concordant monazite ages of the migmatite leucosomes range from 1876 to 1871 Ma (Table 2) and likely correspond to the maximum melting of the Svecofennian rocks. A high water activity in the metamorphic system seems to have been the main factor of intense melting. The age of the widespread stage-2 migmatites corresponded to that of the postgranulite stage.

The identity of the ages of migmatites in the potassic Priozersk and sodic Lahdenpohja migmatite provinces point to the simultaneous (within the error of the dating techniques) development of these migmatites. Practically identical ages were also obtained for monazites from the metamorphic rocks after which migmatites in both zones developed (Table 2). This conclusion finds further support in the similar *P–T* parameters of the metamorphic culminations in these zones. This suggests that the compositional differences between the two migmatite provinces were predetermined by the lateral compositional variability of the supracrustal rocks but not by different endogenic processes in these provinces.

Thus, it was established that metamorphic rocks and migmatites in the Ladoga area show absolutely identical geologic and petrographic characteristics and have the same isotopic ages. This allowed us to reconstruct the succession of Svecofennian endogenic processes

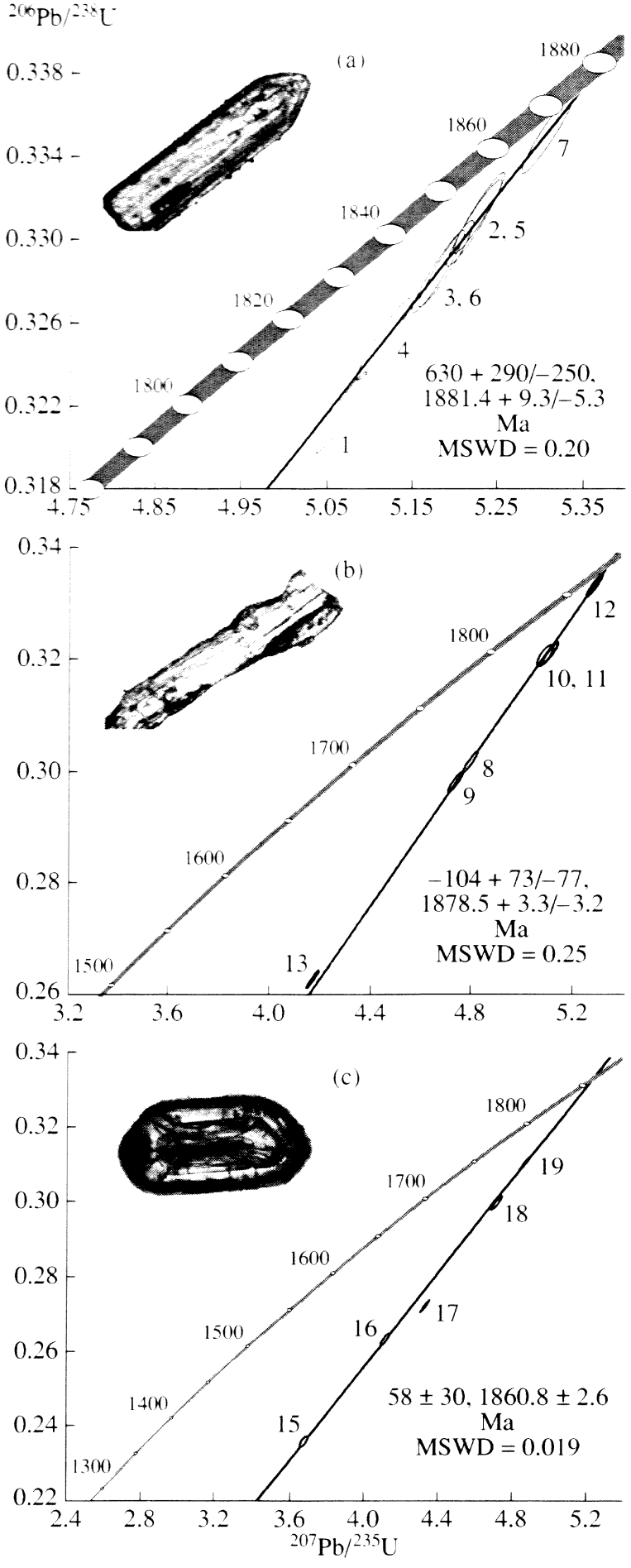

Fig. 6. Concordia plot for zircons from (a) enderbite of the Kurkieki Complex (sample B-99-28), (b) diorite from the Lauvatsaari–Impiniemi Complex (sample B-99-14), and (c) granite of the Tervu Complex (sample B-99-7).

Insets show the most typical types of zircons. Numerals near ellipses are the numbers of the analyzed zircon fractions (Table 2). Regression parameters from (Glebovitsky *et al.*, 2001) are recalculated by the program from (Ludwig, 1998).

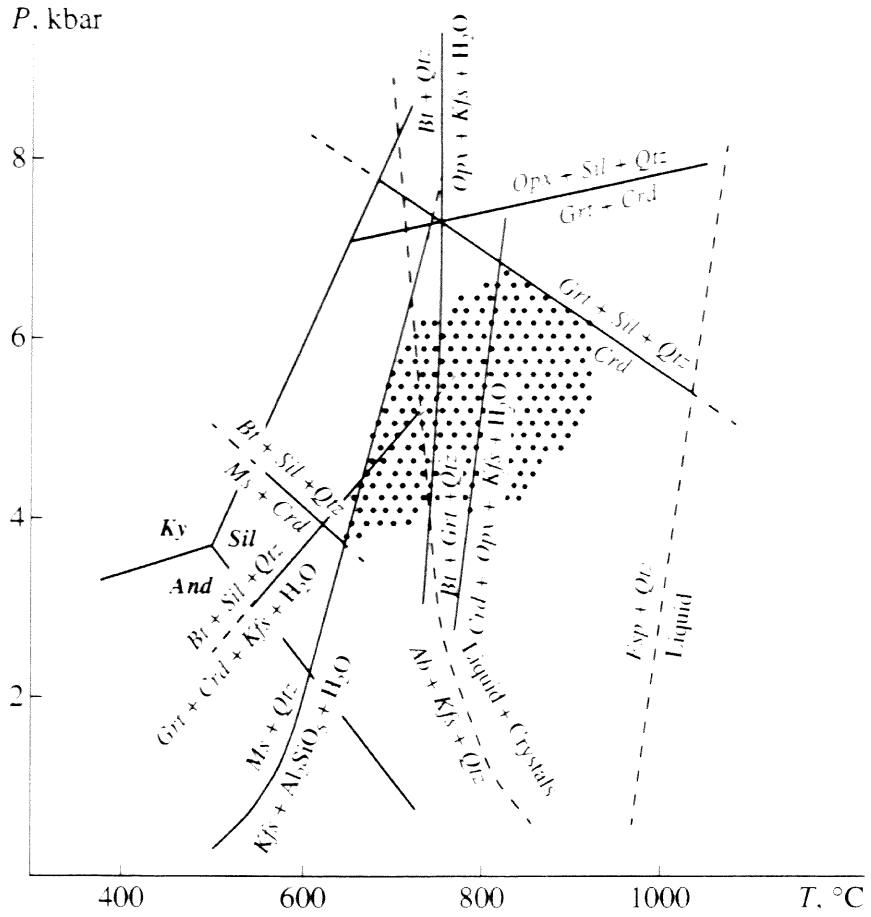

Fig. 7. Metamorphic *P–T* parameters for aluminous rocks from the Priozersk subzone of the high-temperature core of the ZMC. Monovariant reactions were calculated by the TWQ program with the use of the thermodynamic database for granulite assemblages (Berman, 1991; Berman and Aranovich, 1996) and the THERMOCALC program (Powell and Holland, 1998). The dotted area corresponds to the *P–T* parameters determined for the garnet–cordierite assemblages with regard for the position of mineral reactions in (Korikovsky, 1979; Thompson, 1982, 2001). The Al_2SiO_5 triple point is shown according to (Holdaway, 1971).

and their ages in the ZMC core within the age range form 1.88 to 1.85 Ga (Fig. 8).

Magmatic Rocks

The zircon ages of enderbites from the Kurkieki Complex and its analogues in Finland (Kiruversi–Haukiversi Complex) are 1.885–1.870 Ma (Tugarinov and Bibikova, 1980; Korsman *et al.*, 1988). These data and our materials confirm geological observations that the oldest intrusive rocks of the area are metamorphosed norites, enderbites, gabbro, and hyperbasites of the Kurkieki Complex. The hornblende and biotite–hornblende diorites and quartz diorites of the Lauvatsaari–Impiniemi Complex are mostly separated from the enderbites, although their contacts were also observed, a fact testifying to an older age of the diorites. At the same time, the age values presented above indicate that the enderbites and diorites have fairly close ages. Here, the following two considerations should be taken into account. First, as was mentioned above during describing the zircons, the isotopic system of the dated zircons from the enderbites can provide record of postmagmatic alterations, including the recrystallization of the grains during the granulite-facies metamorphism. The widespread association of enderbites and granulite-facies metamorphic rocks and the high-temperature transformations of the enderbites and the intense metamorphic alterations of the zircon suggest that the magmatic crystallization and granulite metamorphism could not have significantly different ages. Second, geological observations are also often consistent with the conclusion about the roughly simultaneous origin of the two complexes: some facies of both the enderbites and the diorites are very similar, perhaps, because these magmatic complexes were produced by the same parental magma.

While the emplacement of the enderbites was related to the granulite stage, the early intermediate stage was marked by the emplacement of diorites and tonalites. Judging from their REE geochemistry, the Lauvatsaari and analogous intrusions resulted from the development of the same mantle magmatic chamber. The mineralogy of the diorites and tonalites implies that their average crystallization temperature was 100°C lower than that of the enderbites. Data on the fluid composition provide grounds to believe that the diorites and, particularly, tonalites crystallized at a higher H_2O fugacity in the fluid (Baltybaev *et al.*, 2000).

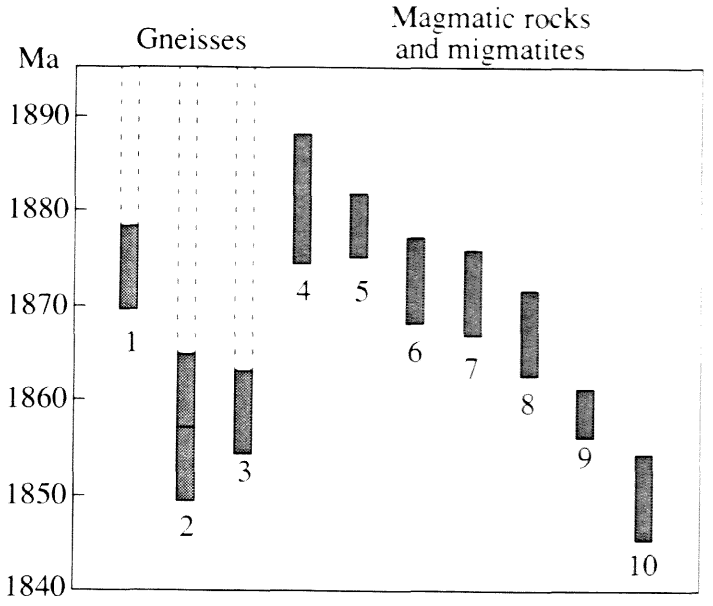

Fig. 8. Genetic succession of rocks inferred from the U–Pb dating of monazite and zircon from various rocks in the Ladoga area.

(1–3) Gneisses: (1) hypersthene–garnet (B-2000-19/1), (2–3) aluminous (B-99-16, B-2000-31); (4–10) intrusive rocks and migmatite leucosomes: (4) enderbite (B-99-28), (5) diorite (B-99-14), (6) leucosome (B-2000-30/1), (7) leucosome (B-2000-19/2), (8) garnet-bearing granite (B-2000-29), (9) granite (B-99-7), (10) granite vein (B-2000-8).

The late intermediate stage was marked by the emplacement of potassic garnet-bearing granites of the Kilpola type. These rocks are particularly rich in fluids, a feature that suggests that the origin of significant volumes of melts with crustal signatures was, perhaps, controlled by the fluid regime (fluid concentrations). Based on the dating of these rocks, the duration of the intermediate metamorphic stage was estimated at approximately 12 ± 7 m.y., which corresponds to the time span starting from the crystallization of the Lauvatsaari intrusion until the emplacement of the garnet granites that marked the end of this stage.

The youngest microcline granites of the Tervu Complex intrude the enderbites and diorites, as well as the metamorphic and ultrametamorphic rocks of the early and intermediate stages. The isochron age of the vein granite facies determines the upper age limit of plutono-metamorphic activity in the Ladoga area. The conclusion that the Tervu Massif was emplaced simultaneously with the late metamorphic processes was drawn based on the kinematic features of the intrusion and related dike and vein series. These rocks are characterized by the gradual loss of plasticity from older to younger members, as is manifested in the transition from weakly plicative to disjunctive features. The duration of the late metamorphic stage was estimated at approximately 17 ± 9 m.y., which corresponds to the time span from the crystallization of the garnet granites to the emplacement of the Tervu intrusion and its final vein facies. The petrochemistry of the granites of this stage indicates that they define an individual evolutionary trend, which is characterized by the development of highly silicic and alkaline magmas (Shul'diner *et al.*, 1997b).

The post-kinematic two-feldspar granites in eastern Finland, which are similar to the Ladoga granites of the Tervu type, were dated at 1810–1830 Ma (Huhma, 1986; Korsman *et al.*, 1988).

CONCLUSIONS

(1) The age of the metamorphic culmination (under granulite-facies conditions) is restricted from below by the age of the supracrustal rocks (1910–1890 Ma). The upper limit is imposed by the emplacement of the diorite massifs that cut the rocks with granulite mineral assemblages (1878.5 ± 3.3 Ma). The enderbite magmatism and related granulite-facies metamorphism were dated at 1881.4 + 9.3/–5.3 Ma. These age limits suggest that the postenderbite granulite metamorphic stage lasted for no more than 15 m.y.

(2) The intermediate metamorphic stage was marked by the emplacement and crystallization of diorite–tonalite massifs with an age of 1878.5 ± 3.3 Ma. This stage was also responsible for the development of migmatites of the second generation, which were dated at 1871–1876 Ma. The intermediate stage ended with the emplacement of potassic garnet-bearing granites with an age of 1866.9 ± 4.4 Ma. Correspondingly, the intermediate amphibolite-facies metamorphic stage lasted for 12 ± 7 m.y.

(3) The final stage of Svecofennian metamorphism in the Ladoga area was associated with the emplacement of late-kinematic granites, which were intruded (together with the vein facies) within the time span of 1860.8 ± 2.6 to 1849.7 ± 4.4 Ma. This late stage was characterized by a temperature decrease from the amphibolite facies to the facies of two-mica gneisses. The stage was the longest and lasted for 17 ± 9 m.y.

(4) The U–Pb ages of migmatites in the potassic and sodic provinces in the area indicate that the leucosomes of all of them developed simultaneously (within the error of the geochronologic techniques). Quite similar ages were also yielded by monazite from the metamorphic protoliths of the migmatites. Thus, the compositional differences between the two migmatite provinces were caused by the lateral compositional variations in the supracrustal rocks but not by different evolution scenarios.

(5) Our data indicate that the total duration of the Svecofennian plutono-metamorphic activity in the high-temperature core of the ZMC of the Ladoga area was no longer than 30–36 m.y.

ACKNOWLEDGMENTS

The authors thank M.D. Tolkachev (Institute of Precambrian Geology and Geochronology, Russian Academy of Sciences) for help in the electron-microscopic

examination of zircon and monazite. We thank E.V. Bibikova (Vernadsky Institute of Geochemistry and Analytical Chemistry, Russian Academy of Sciences) for valuable comments expressed during the reviewing of this manuscript. This study was financially supported by the Russian Foundation for Basic Research (project nos. 02-05-65343, 00-05-65268, 00-05-64897, 00-15-98475, 02-05-64803).

REFERENCES

1. Sh. K. Baltybaev, V. A. Glebovitsky, I. V. Kozyreva, *et al.*, "The Meyeri Trust: The Main Element of the Suture at the Boundary between the Karelian Craton and the Svecofennian Belt in the Ladoga Region of the Baltic Shield," Dokl. Akad. Nauk **348** (3), 353–356 (1996) [Dokl. Earth Sci. **348** (4), 581–584 (1996)].
2. Sh. K. Baltybaev, V. A. Glebovitsky, I. V. Kozyreva, *et al.*, *Geology and Petrology of the Svecofennides in the Ladoga Area* (Izd. S.-Peterburg. Univ., St. Petersburg, 2000) [in Russian].
3. Sh. K. Baltybaev, O. A. Levchenkov, V. A. Glebovitsky, *et al.*, "Dating of High-Aluminous Metamorphic Parageneses in the Potassic Zone of the Ladoga Region of Baltic Shield," Dokl. Akad. Nauk **393** (6), 793–796 (2003) [Dokl. Earth Sci. **393A** (9), 1315–1318 (2003)].
4. R. G. Berman, "Internally Consistent Thermodynamic Data for Minerals in the System Na_2O–K_2O–CaO–MgO–FeO–Fe_2O_3–Al_2O_3–SiO_2–TiO_2–H_2O–CO_2," J. Petrol. **29**, 455–522 (1988).
5. R. G. Berman, "Thermobarometry Using Multiequilibrium Calculations: A New Technique with petrologic Applications," Can. Mineral. **32**, 833–855 (1991).
6. R. G. Berman and L. Y. Aranovich, "Optimized Standard State and Solution properties of Minerals," Contrib. Mineral. Petrol. **126** (1–2), 1–24 (1996).
7. N. G. Berezhnaya, "Criteria of Zircon Genetic Classification in Magmatic Complexes," Dokl. Akad. Nauk **368** (3), 373–376 (1999) [Doklady Earth Sci. **368** (7) 982–984 (1999)].
8. E. V. Bibikova, *Uranium–Lead Geochronology of the Early Evolutionary Stages of Ancient Shields* (Nauka, Moscow, 1989) [in Russian].
9. V. A. Bogachev, V. V. Ivanikov, I. V. Kozyreva, *et al.*, "U–Pb Zircon Dating of Synorogenic Gabbro–Diorite and Granitoid Intrusions in the Northern Ladoga Area," Vestn. S.-Peterburg. Gos. Univ. Ser. 7, No. 3, 23–33 (1999).
10. C. Ehlers, A. Lindroos, and O. Selonen, "The Late Svecofennian Granite-Migmatite Zone of Southern Finland—A Belt of Transpressive Deformation and Granite Emplacement," Precambrian Res. **64**, 295–309 (1993).
11. E. Ekdahl, "Early Proterozoic Karelian and Svecofennian Formations and the Evolution of the Raahe–Ladoga Ore Zone, Based on the Pielavesi Area, Central Finland," Geol. Surv. Finland Bull. **373** (1993).
12. G. Foster, H. Gibson, R. Parrish, *et al.*, "Textural, Chemical and Isotopic Insights into the Nature and Behavior of Metamorphic Monazite," Chem. Geol. **191**, 183–207 (2002).
13. G. Gaal and R. Gorbatschev, "An Outline of the Precambrian Evolution of the Baltic Shield," Precambrian Res. **35** (1), 15–25 (1987).
14. Geologic Evolution of the Deep-Seated Zones of Mobile Belts: Northern Ladoga Area (Nauka, Leningrad, 1970) [in Russian].
15. V. A. Glebovitsky, "Tectonics and Regional Metamorphism in the Early Precambrian of the Eastern Baltic Shield," Region. Geol. Metallogeniya, No. 1, 7–24 (1993).
16. V. A. Glebovitsky, Sh. K. Baltybaev, O. A. Levchenkov, *et al.*, "Main Stage of Plutonic–Metamorphic Activity in the Ladoga Region: Results of Isotopic Age Determinations," Dokl. Akad. Nauk **377** (5), 667–671 (2001) [Dokl. Earth Sci. **377** (3), 302–306 (2001)].
17. J. M. Hanchar and C. E. Miller, "Zircon Zonation Patterns as Revealed by Cathodoluminescence and Backscattered Electron Images: Implication for Interpretation of Complex Crustal Histories," Chem. Geol. **100**, 1–13 (1993).
18. M. J. Holdaway, "Stability of Andalusite and the Aluminum Silicate Phase Diagram," Amer. J. Sci. **271**, 97–131 (1971).
19. H. Huhma, "Sm-Nd, Pb and Pb-Pb Isotopic Evidence for the Origin of the Early Proterozoic Svecofennian Crust in Finland," Geol. Surv. Finland Bull. **337** (1986).
20. H. Huhma, S. Claesson, P. D. Kinny, and I. S. Williams, "The Growth of the Early Proterozoic Crust: New Evidence from Svecofennian Detrital Zircon," Terra Nova **3** (2), 175–179 (1991).
21. V. V. Ivanikov, D. L. Konopel'ko, Yu. D. Pushkarev, *et al.*, "Apatite-Bearing Ultramafic–Mafic Rocks of the Ladoga Area," Vestnik S.-Peterburg. Gos. Univ., Ser. 7, No. 4, 76–81 (1996).
22. Y. Kahkonen, H. Huhma, and K. Aro, "U–Pb Ages and Rb–Sr Whole Rock Isotope Studies of Early Proterozoic Volcanic and Plutonic Rocks Near Tampere, Southern Finland," Precambrian Res. **45** (1-3), 27–42 (1989).
23. A. N. Kazakov, *Deformations and Overprinted Folding in Metamorphic Complexes* (Nauka, Leningrad, 1976) [in Russian].
24. V. I. Kitsul, *Petrology of Carbonate Rocks in the Ladoga Formation* (Izd. Akad. Nauk SSSR, Moscow, 1963) [in Russian].
25. K. Korsman, P. Hollts, T. Hautala, and P. Wasenius, "Metamorphism as an Indicator of the Evolution and Structure of the Crust in Eastern Finland," Geol. Surv. Finland Bull. **328** (1984).
26. K. Korsman, R. Niemela, and P. Wasenius, "Multistage Evolution of the Proterozoic Crust at the Savo Schist Belt, Eastern Finland," Geol. Surv. Finland Bull. **343**, 89–96 (1988).
27. A. B. Kotov, E. V. Bibikova, L. A. Neimark, *et al.*, "Duration of Tectono-Metamorphic Cycles," in *Structural Analysis of Crystalline Complexes* (Irkutsk, 1992), pp. 19–20 [in Russian].
28. A. B. Kotov and L. M. Samorukova, *Evolution of Granite Formation during Early Precambrian Tectono-Metamorphic Cycles: Evidence from Structural-Petrographic and Fluid Inclusion Studies* (Nauka, Leningrad, 1990) [in Russian].

29. D. Konopelko, O. Eklund, and V. Ivanikov, "1.8 Ga Phosphorus-Rich Lamprophyre–Granitoid Complex in the Fennoscandian Shield: Parental Magmas and Fractionation Paths," Acta Universitatis Carolinae—Geologica. **42** (1), 51–54 (1998).

30. S. P. Korikovsky, *Metamorphic Facies of Metapelites* (Nauka, Moscow, 1979) [in Russian].

31. T. E. Krogh, "A Low Contamination Method for Hydrothermal Decomposition of Zircon and Extraction of U and Pb for Isotopic Determination," Geochim. Cosmochim. Acta. **37**, 485–494 (1973).

32. R. Lahtinen, "Crustal Evolution of the Svecofennian and Karelian Domains during 2.1–1.79 Ga, with Special Emphasis on the Geochemistry and Origin of 1.93–1.91 Gneiss Tonalites and Associated Supracrustal Rocks in the Rautalampi Area, Central Finland," Geol. Surv. Finland. Bull. **378**, 128 (1994).

33. S. B. Lobach-Zhuchenko, V. P. Chekulaev, and V. S. Baikova, *Epochs and Types of Granite Formation in the Precambrian of the Baltic Shield* (Nauka, Leningrad, 1974) [in Russian].

34. K. R. Ludwig, "A Computer Program for Proceeding Pb–U–Th Isotopic Data," US Geol. Surv. Open-File Rep., 91–445 (1991).

35. K. R. Ludwig, "Isoplot/Ex. Version 1.00," Berkeley Geochronology Center. Special Publication, No. 1, 1–43 (1998).

36. *Migmatization and Granite Formation at Different Thermodynamic Regimes* (Nauka, Leningrad, 1985) [in Russian].

37. A. Moeller, U. Poller, A. Kennedy, and A. Kzoener, "Trace and Rare Element Geochemistry of Magmatic and Metamorphic Zircon: Caveats for Geochronological Interpretation Based on Th/U and Morphology Only," (EUG, Strasbourg, 2001), p. 6568.

38. Yu. A. Morozov and D. E. Gaft, On the Nature of Granite–Gneiss Domes in the Northern Ladoga Area," in *Structure and Petrology of Precambrian Complexes* (Nauka, Moscow, 1985), pp. 3–100 [in Russian].

39. H. Mouri, K. Korsman, and H. Huhma, "Tectono-Metamorphic Evolution and Timing of the Melting Processes in the Svecofennian Tonalite–Trondhjemite Migmatite Belt: An Example from Luopioinen, Tampere Area, Southern Finland," Geol. Soc. Bull. **71**, 31–56 (1999).

40. Yu. V. Nagaitsev, *Petrology of Metamorphic Rocks of the Ladoga and Belomorian Complexes* (Izd. Leningrad. Gos. Univ., Leningrad, 1974) [in Russian].

41. A. A. Predovskii, V. P. Petrov, and O. A. Belyaev, *Geochemistry of Ore Elements in Precambrian Metamorphic Series* (Nauka, Leningrad, 1967) [in Russian].

42. Yu. D. Pushkarev and G. I. Ryungenen, "Sr and Pb Isotopic Compositions of Subalkaline Ultramafic and Mafic Rocks of the Elisenvaari Complex with Reference to the Identification of the Source of the Parental Melts," in *Proceedings of 14th Symp. on Isotopic Geochemistry* (Moscow, 1995), pp. 30–31.

43. L. J. Pekkarinen and H. Lukkarinen, "Paleoproterozoic Volcanism in Kiihtelisvaara–Tohmajarvi District, Eastern Finland," Geol. Surv. Finland Bull. **357** (1991).

44. R. Powell and T. J. Holland, J. "An Internally Consistent Thermodynamic Dataset with Uncertainties and Correlations," J. Metamorph. Geology., No. 6, 173–204 (1998).

45. D. Rubatto, I. S. Williams, and I. S. Buick, "Zircon and Monazite Response to Prograde Metamorphism in the Reynolds Range, Central Australia," Contrib. Mineral. Petrol. **140**, 458–468 (2001).

46. G. M. Saranchina, *Precambrian Granitoid Magmatism and Metamorphism: Examples of the Ladoga and Other Areas* (Nauka, Leningrad, 1972) [in Russian].

47. U. Schaltegger, C. M. Fanning, D. Guenther, *et al.*, "Growth, Annealing, and Crystallization of Zircon and Preservation of Monazite in High-Grade Metamorphism: Conventional and *In-Situ* U–Pb Isotope, Cathodolumenescence, and Microchemical Evidence," Contrib. Mineral. Petrol. **134**, 186–201 (1999).

48. I. S. Sedova, S. A. Vasil'eva, and E. N. Trunova, "K-Feldspar Composition in Migmatites of the Ladoga Complex," Zap. Vses. Mineral. O–va, No. 2, 93–104 (1989).

49. V. I. Shul'diner, Sh. K. Baltybaev, and I. V. Kozyreva, "Tectono-Metamorphic Zoning of the Ladoga Area," Vestnik S.-Peterburg. Gos. Univ., Ser. 7, No. 3, 63–70 (1997a).

50. V. I. Shul'diner, Sh. K. Baltybaev, and I. V. Kozyreva, "Metamorphic Evolution of Garnet-Bearing Granulites in the Western Ladoga Area," Petrologiya **5** (3), 253–277 (1997b) [Petrology **5** (3), 223–245 (1997)].

51. V. I. Shul'diner, I. V. Kozyreva, and Sh. K. Baltybaev, "Geochronology and Formation Subdivisions of the Lower Precambrian in the Northwestern Ladoga Region," Stratigr. Geol. Korrelyatsiya **4** (3), 11–22 (1996) [Stratigr. Geol. Corr. **4** (3), 220–230 (1996)].

52. V. I. Shul'diner, O. A. Levchenkov, S. Z. Yakovleva, *et al.*, "Upper Karelian in the Stratigraphic Chart of Russia: Selection of the Lower Boundary and Regional Subdivisions of the Stratotypical Area," Stratigr. Geol. Korrelyatsiya **8** (6), 20–33 (2000) [Stratigr. Geol. Corr. **8** (6), 544–556 (2000)].

53. A. Simonen, "The Precambrian of Finland," Geol. Surv. Finland Bull. **304** (1980).

54. N. G. Sudovikov, "Migmatites: Genesis and Study Methods," in *Trudy Lab. Geol. Dokembriya* (Izd-vo AN SSSR, Leningrad, 1955), pp. 97–173 [in Russian].

55. A. P. Svetov and L. P. Sviridenko, *The Sortavala Svecokarelian Group in the Ladoga Area* (Karel'skii Nauch. Tsentr Ross. Akad. Nauk, Petrozavodsk, 1992) [in Russian].

56. A. B. Thompson, "Dehydration Melting of Pelitic Rocks and the Generation of H_2O-Undersaturated Granitic Liquids," Am. J. Sci., 1567–1595 (1982).

57. A. B. Thompson, "Clockwise *P–T* Paths for Crustal Melting and H_2O Recycling in Granite Source Regions and Migmatite Terrains," Lithos. **56** (1), 33–45 (2001).

58. A. I. Tugarinov and E. V. Bibikova, *Zircon Geochronology of the Baltic Shield* (Nauka, Moscow, 1980) [in Russian].

59. M. Vaasjoki and O. T. Rämö, "New Zircon Age Determinations from the Wiborg Rapakivi Batholith, Southern Finland," Geol. Surv. Finland Spec. Pap., No. 8 (1989).

60. M. Vaisanen, I. Manttari, and P. Holtta, "Svecofennian Magmatic and Metamorphic Evolution in Southwestern Finland as Revealed by U–Pb zircon SIMS Geochronology," Precambrian Res. **116**, 111–127 (2002).